Nuclear Instruments and Methods in Physics Research A 613 (2010) 245–250

Contents lists available at ScienceDirect

Nuclear Instruments and Methods in Physics Research A

journal homepage: www.elsevier.com/locate/nima

# Long-term determination of airborne concentrations of unattached and attached radon progeny using stacked LR 115 detector with multi-step etching

D. Nikezic, K.N. Yu *

*Department of Physics and Materials Science, City University of Hong Kong, Tat Chee Avenue, Kowloon Tong, Kowloon, Hong Kong*

ARTICLE INFO

*Article history:*
Received 5 September 2009
Received in revised form
10 November 2009
Accepted 16 November 2009
Available online 24 November 2009

*Keywords:*
SSNTDs
Nuclear track detectors
Long-term measurements
Radon progeny

ABSTRACT

We developed the theoretical basis for long-term determination of airborne concentrations of unattached and attached radon progeny. The work was separated into two parts. First, we showed that (stacked and multiply etched) LR 115 detectors could be used to determine airborne concentrations of the short-lived radon progeny, $^{218}$Po and $^{214}$Bi. The equilibrium factor $F$ between radon and its progeny could then be determined through the use of the reduced equilibrium factor $F_{red}$. The airborne concentrations of $^{214}$Pb could then be determined. Second, we developed a method based on the airborne concentrations of $^{218}$Po, $^{214}$Pb and $^{214}$Bi to determine the parameters of the Jacobi room model, viz., the ventilation rate $\lambda_v$, aerosol attachment rate $\lambda_a$, deposition rate of unattached progeny $\lambda_d{}^u$ and the deposition rate of attached progeny $\lambda_d{}^u$. With these parameters, the unattached fraction $f_p$ of the potential alpha energy concentration could also be determined. Knowledge of $f_p$, together with $F$, would enable more accurate determination of the effective dose in the human lung.



## 1. Introduction

Epidemiological studies have provided reasonably firm estimates of the risk of radon-induced lung cancers. It is well established that the effective dose in the lung is mainly due to short-lived radon progeny, i.e., $^{218}$Po, $^{214}$Pb, $^{214}$Bi and $^{214}$Po, but not the radon ($^{222}$Rn) gas itself. Accordingly, long-term measurements of the concentrations of radon progeny or the equilibrium factor $F$, the size distribution of radon progeny and the unattached fraction $f_p$ of the potential alpha energy concentration are needed to accurately assess the health hazards contributed by radon progeny. The equilibrium factor $F$ between radon and its progeny is defined as $F=0.105f_1+0.515f_2+0.380f_3$ where $f_i$ is the ratio of the activity concentration $C_i$ of the $i$th radon progeny to the activity concentration $C_0$ of $^{222}$Rn. Here, $i=1$ stands for $^{218}$Po, $i=2$ for $^{214}$Pb and $i=3$ for $^{214}$Bi (or $^{214}$Po, because $^{214}$Bi and $^{214}$Po are in secular equilibrium).

Nowadays, in general practice, the radon gas concentration is first determined and an assumed $F$ between radon and its progeny, typically from 0.4 to 0.5, is then applied. The exposure to radon progeny can be expressed in the traditional unit *working level month* (WLM) and then multiplied by the dose conversion factor (DCF) by assuming a given aerosol size distribution to give the effective dose. However, in reality, the concentrations of radon and its progeny vary significantly with time and place, and an assumed $F$ cannot reflect the actual conditions [1]. This problem cannot be solved through active measurements based on air filtering, since they only give short-term measurements. Moreover, $f_p$ can potentially have a large contribution to the effective dose (or the DCF), so it seems pertinent to measure or estimate $f_p$ correctly for realistic determination of the effective lung dose.

In the present work, we developed the theoretical basis for long-term determination of airborne concentrations of unattached and attached radon progeny (i.e., both $F$ and $f_p$ will be determined). The work was separated into two parts.

First, we showed that (stacked and multiply etched) LR 115 detectors could be used for long-term measurements of the equilibrium factor $F$ between radon and its progeny. Researchers have proposed different long-term methods for measuring radon progeny concentrations [2–10]. Unfortunately, many of these proposed methods suffer from some kinds of problems. Recent reviews of the methods have been given in Refs. [11–13]. A pioneering method that was feasible for long-term measurements of $F$ through the so-called "reduced equilibrium factor" $F_{red}$, the latter being defined as $F_{red}=0.105f_1+0.380f_3$, was proposed in Ref. [11]. The method involved separate measurements of $f_1$ and $f_3$. Associated with the method, two bare Makrofol detectors with carefully chosen electrochemical etching conditions were proposed to provide different energy windows, i.e., different upper and lower alpha-particle energy thresholds, to obtain the airborne

* Corresponding author. Tel.: +852 27887812; fax: +852 27887830.
*E-mail address:* peter.yu@cityu.edu.hk (K.N. Yu).

0168-9002/$ - see front matter © 2009 Elsevier B.V. All rights reserved.
doi:10.1016/j.nima.2009.11.058

**Table 1**
Ranges for the parameters of the Jacobi model employed for the computer simulations in Ref. [11] and in the present work.

| Parameter | Lower limit | Upper limit |
|---|---|---|
| Ventilation rate $\lambda_v$ | 0.2 | 2.1 |
| Aerosol attachment rate $\lambda_a$ | 5 | 500 |
| Deposition rate of unattached progeny $\lambda_d{}^u$ | 5 | 110 |
| Deposition rate of attached progeny $\lambda_d{}^a$ | 0.05 | 1.1 |

$^{218}$Po and $^{214}$Po concentrations [11]. A third Makrofol detector was used inside a diffusion chamber to measure the activity concentration of $^{222}$Rn. It can be shown that the $F$ depended on $F_{red}$ in a very good manner. This relationship was established through the Jacobi room model. Four parameters are involved in this model, namely, the ventilation rate $\lambda_v$, aerosol attachment rate $\lambda_a$, deposition rate of unattached progeny $\lambda_d{}^u$ and the deposition rate of attached progeny $\lambda_d{}^a$. The ranges for these parameters employed for the computer simulations are shown in Table 1. Combinations of these parameters were randomly sampled from these ranges, and for each of these combinations, the concentrations of radon and its progeny were calculated.

Despite the enlightening idea of the method, the requirement to employ the relatively sophisticated electrochemical etching of Makrofol detectors, together with the narrow energy windows required might have hindered the method from reaching the popularity it should deserve. In view of this, we are proposing in the present work to use the more commonly used LR 115 solid-state nuclear track detectors (SSNTDs) instead of the Makrofol detectors to determine $F_{\mathrm{red}}$. In the present paper, a theoretical basis for a method based on multi-step etching of stacked LR 115 SSNTDs for long-term measurements of the airborne concentrations of the two alpha-particle emitting radon progeny (namely, $^{218}$Po and $^{214}$Po) is first developed, which will be presented in Section 2. The equilibrium factor $F$ between radon and its progeny could then be determined through the use of the reduced equilibrium factor $F_{red}$. The airborne concentrations of $^{214}$Pb could then be determined.

In the second part, we developed a method based on the airborne concentrations of $^{218}$Po, $^{214}$Pb and $^{214}$Bi to determine the parameters of the Jacobi room model, i.e., $\lambda_v$, $\lambda_a$, $\lambda_d{}^u$ and $\lambda_d{}^a$. These procedures will be described in Section 3. With these parameters, the unattached fraction $f_p$ of the potential alpha energy concentration could also be determined. Knowledge of $f_p$, together with $F$, would enable more accurate determination of the effective dose in the human lung.

In the outset, it is here remarked that the present method is applicable only when neglecting the contribution of thoron and its progeny. Although high thoron gas concentrations are not commonly encountered, it will be prudent to always measure the thoron gas concentrations along with the radon gas concentrations, e.g., through the twin diffusion chamber measurements.

## 2. Determination of $f_i$ from multi-step etching of stacked LR 115 SSNTDs

### 2.1. Model

The experimental setup, which is considered in the present paper, consists of one detector enclosed in a diffusion chamber for the measurement of $^{222}$Rn only, and two stacked active layers of LR 115 detectors, as shown in Fig. 1. An extra detector in a separate

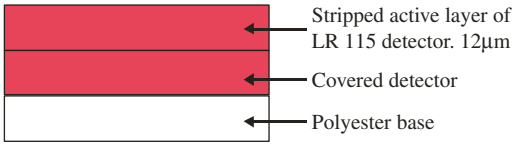


**Fig. 1.** Schematic diagram of the stacked LR 115 detectors, with a stripped active layer of an LR 115 detector stacked on top of another LR 115 detector.

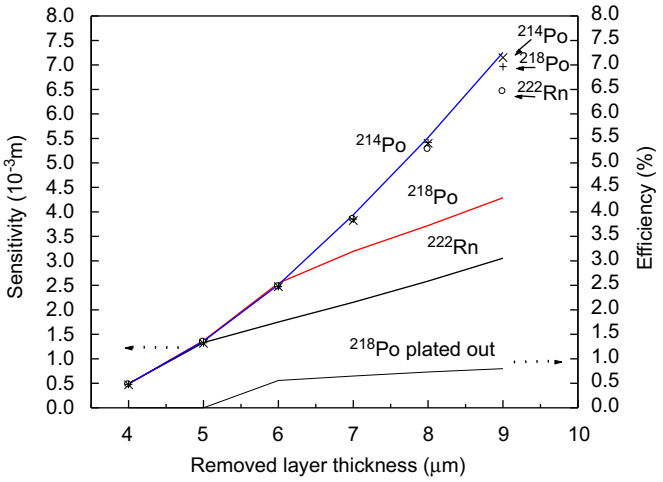


**Fig. 2.** Sensitivity of the covered detector to $^{222}$Rn, $^{218}$Po and $^{214}$Po as represented by solid lines (referred to by the left axis). The sensitivities for the bare detector as represented by scattered points (also referred to by the left axis). Detection efficiency (in %) for plateout $^{218}$Po is referred to by the right axis.

diffusion chamber is optional to provide measurements on $^{222}$Rn and $^{220}$Rn simultaneously (through the so-called twin diffusion chamber method). A similar setup of stacked LR 115 detectors has recently been used for another purpose, viz., in retrospective radon progeny measurements through measurements of $^{210}$Po activities on glass objects using stacked LR 115 detectors [14].

For the stacked combination, a stripped active layer will operate as a bare (or open) detector; the responses of the bare LR 115 detector to $^{222}$Rn, $^{218}$Po and $^{214}$Po are expressed by the partial sensitivities $\varepsilon_i$ of the detector to these radionuclides (i.e., the number of tracks per unit area per unit exposure, in the unit $(\mathrm{m}^{-2})/(\mathrm{Bqm}^{-3}\,\mathrm{s})$ or just $(m)$). The partial sensitivities $\varepsilon_i$ were found to be the same for $^{222}$Rn, $^{218}$Po and $^{214}$Po [12]. The equality of partial sensitivities arises from the presence of the lower and upper energy thresholds (which is well below 5.49 MeV) for track formation in the LR 115 detector. The equality is impaired for very large removed layers; in fact the partial sensitivities start to differ when the removed layer is 9 μm, as can be seen in Fig. 2. When the removed layer increases, the energy window expands. When the removed layer is larger than 9 μm, the upper energy threshold exceeds 5.49 MeV. The reason behind the equality of partial sensitivities is then no longer valid, and the partial sensitivities start to differ from one another. For removed layers smaller than 9 μm, the partial sensitivities are equal and we can write $\varepsilon_i = \varepsilon_{^{222}\mathrm{Rn}} = \varepsilon_{^{218}\mathrm{Po}} = \varepsilon_{^{214}\mathrm{Po}}$. The total track density $\rho$ (in track/m$^2$) on the bare detector is therefore

$$\rho = \varepsilon_i(C_0 + C_1 + C_3)t \tag{1}$$

where $t$ is the exposure time and $C_3 = C_4$. The presence of the energy window for alpha-particle detection in the LR 115 detector has led to the relationship shown in Eq. (1).

Polyallyldiglycol carbonate, which is another popular SSNTD used for radon measurements and commonly marketed as CR-39, as well as other SSNTDs do not have such an appropriate energy window so Eq. (1) will not be valid in these cases.

Below the stripped active layer is the covered detector, which is in fact the active layer intact with its polyester base. The track densities (in $track \cdot m^{-2}$) on the covered detector for a removed layer $h_1$ are

$$\rho_c^1 = (\varepsilon_0^1 C_0 + \varepsilon_1^1 C_1 + \varepsilon_3^1 C_3 + \varepsilon_{1p}^1 C_{1p})t \quad (2)$$

and similarly for a removed layer $h_2$

$$\rho_c^2 = (\varepsilon_0^2 C_0 + \varepsilon_1^2 C_1 + \varepsilon_3^2 C_3 + \varepsilon_{1p}^2 C_{1p})t \quad (3)$$

where $\varepsilon_i{}^1$ are the sensitivities for the removed layer $h_1$ and $\varepsilon_i{}^2$ for the removed layer $h_2$; $\varepsilon_{1p}{}^1$ and $\varepsilon_{1p}{}^2$ are the sensitivities to plateout $^{218}$Po ($C_{1p}$) for the two removed layers. The covered detector can detect plateout because the alpha particles emitted just above the bare detector will lose sufficient energy (in the bare detector) so that their energies will fall below the upper energy threshold of the covered detector.

In Eqs. (2) and (3), the unknown variables are $C_1$, $C_3$ and $C_{1p}$. From these, $C_{1p}$ can be eliminated, and one equation with the unknowns $C_1$ and $C_3$ is obtained.

### 2.2. Partial sensitivities

The partial sensitivities were calculated with programs developed earlier [12], of which the description will not be repeated here. In these calculations, the most important information is the $V$ function, which is given by the ratio of the track etch rate $V_t$ to the bulk etch rate $V_b$, i.e., $V = V_t/V_b$. Here, the $V$ function obtained in [15,16] will be employed

$$V = 1 + (A_1 e^{-A_2 X} + A_3 e^{-A_4 X})(1 - e^{-X}) \quad (4)$$

where $X$ is the residual range of alpha particles and the constants are $A_1 = 14.50$, $A_2 = 0.50$, $A_3 = 3.9$ and $A_4 = 0.066$.

The results of calculations are presented in Fig. 2, where the partial sensitivities to $^{222}$Rn, $^{218}$Po and $^{214}$Po of the covered detector (shown as solid lines), and those of the bare detector (shown as scattered points) are referred to by the left ordinate axis, while the efficiency to plateout $^{218}$Po is referred to by the right ordinate axis.

Several interesting observations are seen in Fig. 2:

(1) The sensitivities of the bare detector to different alpha-particle emitters in the $^{222}$Rn chain are equal to one another for removed layers below 8 μm. This agreed with our previous results [12].
(2) The sensitivity of the covered detector to $^{214}$Po is just equal to the sensitivity of the bare detector (note that the line that represents the sensitivity of the covered detector passes through the points, which represent those for the bare detector). Some discrepancies between the sensitivities for the bare and covered detectors for detection of $^{214}$Po occur beyond the removed layer of 9 μm.
(3) The efficiency of the covered detector to the deposited $^{218}$Po is less than 10% and it only changes slightly for removed layers between 6 and 9 μm. For removed layers below 5 μm, plateout is not detected. The efficiency of the covered detector to plateout $^{214}$Po is equal to 0 because the thickness (12 μm) of the open stripped active layer is not enough to reduce the energy of alpha particles from 7.69 MeV to below the upper energy threshold of detection.

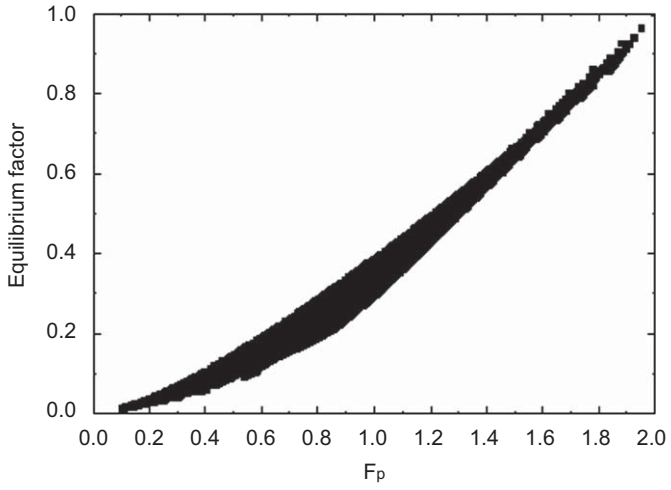


**Fig. 3.** Dependence of the equilibrium factor $F$ on the proxy equilibrium factor $F_p$ ($=f_1+f_3$) (from Ref. [13]).

### 2.3. Methodology

After elimination of $C_{1p}$ from Eqs. (2) and (3), we obtain

$$C_1\left(\varepsilon_1^2 - \frac{\varepsilon_{1p}^2}{\varepsilon_{1p}^1}\varepsilon_1^1\right) + C_3\left(\varepsilon_3^2 - \frac{\varepsilon_{1p}^2}{\varepsilon_{1p}^1}\varepsilon_3^1\right) = \frac{\rho_c^2}{t} - \frac{\varepsilon_{1p}^2}{\varepsilon_{1p}^1}\frac{\rho_c^1}{t} - C_0\left(\varepsilon_0^2 - \frac{\varepsilon_{1p}^2}{\varepsilon_{1p}^1}\varepsilon_0^1\right) \quad (5)$$

We can express the response of the bare detector in the form

$$C_1 + C_3 = \frac{\rho}{\varepsilon_i t} - C_0 \quad (6)$$

Eqs. (5) and (6) then form a system of two equations with two unknown variables, $C_1$ and $C_3$. It is assumed that $C_0$ is known from the readings from the detector exposed within the diffusion chamber (or from some other forms of measurements). In principle, this approach should enable determination of $C_1$ and $C_3$.

Eq. (5) can be further simplified as follows. If the removed layer is larger than 6.5 μm, $\varepsilon_p$ is almost constant, as can be seen in Fig. 2. In such cases, $\varepsilon_{1p}{}^1 \approx \varepsilon_{1p}{}^2$ and Eq. (5) becomes

$$C_1(\varepsilon_1^2 - \varepsilon_1^1) + C_3(\varepsilon_3^2 - \varepsilon_3^1) = \frac{\rho_c^2}{t} - \frac{\rho_c^1}{t} - C_0(\varepsilon_0^2 - \varepsilon_0^1) \quad (7)$$

From Eq. (6)

$$C_3 = \frac{\rho}{\varepsilon_i t} - C_0 - C_1$$

By substituting this into Eq. (7), the equation for $C_1$ is obtained as

$$C_1(\varepsilon_1^2 - \varepsilon_1^1) + \left(\frac{\rho}{\varepsilon_i t} - C_0 - C_1\right)(\varepsilon_3^2 - \varepsilon_3^1) = \frac{\rho_c^2}{t} - \frac{\rho_c^1}{t} - C_0(\varepsilon_0^2 - \varepsilon_0^1) \quad (8)$$

or

$$C_1 = \frac{((\rho_c^2 - \rho_c^1)/t) - C_0(\varepsilon_0^2 - \varepsilon_0^1) - ((\rho/\varepsilon_i t) - C_0)(\varepsilon_3^2 - \varepsilon_3^1)}{(\varepsilon_1^2 - \varepsilon_1^1) - (\varepsilon_3^2 - \varepsilon_3^1)} \quad (9)$$

Finally, $C_3$ is obtained as

$$C_3 = \frac{\rho}{\varepsilon_i t} - C_0 - \frac{((\rho_c^2 - \rho_c^1)/t) - C_0(\varepsilon_0^2 - \varepsilon_0^1) - ((\rho/\varepsilon_i t) - C_0)(\varepsilon_3^2 - \varepsilon_3^1)}{(\varepsilon_1^2 - \varepsilon_1^1) - (\varepsilon_3^2 - \varepsilon_3^1)} \quad (10)$$

On getting $C_1$ and $C_3$, and knowing $C_0$, we obtain $f_1$ and $f_3$, and thus $F_{red}$ given by $F_{red} = 0.105 f_1 + 0.380 f_3$ (Fig. 3).

### 2.4. Determination of $f_2$

The methodology above enabled the determination of $f_1$ and $f_3$. However, $f_2$ is undetermined. Fortunately, the relationship

between $F$ and $F_{red}$ enables determination of $F$ with relatively small uncertainties, so it is possible to determine $f_2$ also with relatively small uncertainties when $f_1$ and $f_3$ are known. From the best linear fit $F=2.107F_{red}$ and from Eq. (1), we have

$$f_2 \approx 2.15\,F_{red} \tag{11}$$

## 3. Determination of airborne concentrations of individual short-lived radon progeny

Knowledge of airborne concentrations of individual short-lived radon progeny will undoubtedly enable more accurate determination of the effective dose in the human lung, than the knowledge of only $F$. This is manifested in the potentially large contribution of $f_p$ to the effective dose (or the dose conversion factor DCF). We here take a nominal case where $F=0.372$ as our example, and perform calculations with our own computer program LUNGDOSE.F90 described in Ref. [17]. The DCF will be equal to 13.03 and 18.57 mSv/WLM for $f_p=0.0343$ and 0.196, respectively. The need to correctly measure or estimate $f_p$ seems pertinent for the realistic determination of the effective lung dose.

We define the unattached and the attached parts of the activity concentrations ($C_1$, $C_2$, $C_3$) as ($C_1^u$, $C_2^u$, $C_3^u$) and ($C_1^a$, $C_2^a$, $C_3^a$), respectively. Correspondingly, the unattached and the attached parts of the ratios ($f_1$, $f_2$, $f_3$) are ($f_1^u$, $f_2^u$, $f_3^u$) and ($f_1^a$, $f_2^a$, $f_3^a$), respectively.

### 3.1. Simplification: introduction of aggregate deposition rate

The known variables are now the activity concentrations of $C_0$, $C_1$, $C_2$ and $C_3$ ($=C_4$). The task here is to estimate $C_i^u$ and $C_i^a$ (or equivalently $f_i^u$ and $f_i^a$) to enable more accurate determination of the effective dose. Here, the unknown variables are ($C_1^u$, $C_2^u$, $C_3^u$) and ($C_1^a$, $C_2^a$, $C_3^a$). All these can be calculated if the parameters of the Jacobi model [18] are known. The Jacobi model is presented by the following set of equations:

$$C_1^u = \frac{\lambda_1 C_0}{\lambda_1+\lambda_v+\lambda_a+\lambda_d^u}, \quad C_1^a = \frac{\lambda_a C_1^u}{\lambda_1+\lambda_v+\lambda_d^a} \tag{12a}$$

$$C_2^u = \frac{\lambda_2(C_1^u+p_1C_1^a)}{\lambda_2+\lambda_v+\lambda_a+\lambda_d^u}, \quad C_2^a = \frac{\lambda_a C_2^u+(1-p_1)\lambda_2 C_1^a}{\lambda_2+\lambda_v+\lambda_d^a} \tag{12b}$$

$$C_3^u = \frac{\lambda_3 C_2^u}{\lambda_3+\lambda_v+\lambda_a+\lambda_d^u}, \quad C_3^a = \frac{\lambda_3 C_2^a+\lambda_a C_3^u}{\lambda_3+\lambda_v+\lambda_d^a} \tag{12c}$$

where $\lambda_1$, $\lambda_2$ and $\lambda_3$ are the physical decay constants of $^{218}$Po, $^{214}$Pb and $^{214}$Bi, respectively, and $p_1$ is the recoil factor (0.83). The concentrations of the progeny are the sum of corresponding concentrations in the unattached and attached modes, i.e.,

$$C_1 = C_1^u + C_1^a, \;\; C_2 = C_2^u + C_2^a, \;\; C_3 = C_3^u + C_3^a \tag{13}$$

The ratios $f_i^u$ and $f_i^a$ are defined as follows:

$$f_i^u = C_i^u/C_0, \;\; f_i^a = C_i^a/C_0, \;\; f_i = C_i/C_0 \quad (i=1,2,3). \tag{14}$$

We first attempt to simplify Eqs. (12a)–(12c) for the Jacobi model by introducing the "*aggregate*" deposition rate. Under such a scenario, we modify Eqs. (12a)–(12c) as follows. The concentration of $^{218}$Po ($C_1$) is equal to

$$C_1 = \frac{\lambda_1 C_0}{\lambda_1+\lambda_v+\lambda_{d1}} = \frac{\lambda_1 C_0}{\lambda_1+r_1}. \tag{15}$$

where $\lambda_{d1}$ is the aggregate deposition rate of $^{218}$Po (aggregate for both unattached and attached progeny). The term $r_1$ is the total removal rate of $^{218}$Po by ventilation and deposition. Note that $\lambda_1+r_1$ is total removal rate of $^{218}$Po by all processes, including the radioactive decay. It will be shown that the aggregate deposition rate is given as

$$\lambda_{d1} = \frac{\lambda_d^u C_1^u + \lambda_d^a C_1^a}{C_1} = \frac{\lambda_d^u f_1^u + \lambda_d^a f_1^a}{f_1} \tag{16}$$

To derive the above expression for $\lambda_{d1}$, we calculate $\lambda_{d1}$ from Eq. (15) and combine it with the first equation in Eq. (13) as

$$\begin{aligned}\lambda_{d1} &= \frac{\lambda_1 C_0}{C_1} - \lambda_1 - \lambda_v = \frac{\lambda_1}{f_1} - \lambda_1 - \lambda_v \\ &= \frac{\lambda_1 - \lambda_1 f_1 - \lambda_v f_1}{f_1} = \frac{\lambda_1 - \lambda_1(f_1^u+f_1^a) - \lambda_v(f_1^u+f_1^a)}{f_1} \\ &= \frac{\lambda_1 - (\lambda_1+\lambda_v)f_1^u - (\lambda_1+\lambda_v)f_1^a}{f_1}\end{aligned}$$

From the first equation in Eq. (12a), we have

$$f_1^u = \frac{\lambda_1}{\lambda_1+\lambda_v+\lambda_a+\lambda_d^u} \Rightarrow (\lambda_1+\lambda_v)f_1^u = \lambda_1 - f_1^u\lambda_a - f_1^u\lambda_d^a$$

From the second equation in Eq. (12a), we have

$$f_1^a = \frac{\lambda_a f_1^u}{\lambda_1+\lambda_v+\lambda_d^a} \Rightarrow (\lambda_1+\lambda_v)f_1^a = \lambda_a f_1^u - f_1^a\lambda_d^a$$

Substituting these expressions into the expression for $\lambda_{d1}$, we have

$$\begin{aligned}\lambda_{d1} &= \frac{\lambda_1 - (\lambda_1+\lambda_v)f_1^u - f_1^a(\lambda_1+\lambda_v)}{f_1} \\ &= \frac{\lambda_1 - \lambda_1 + f_1^u\lambda_a + f_1^u\lambda_d^a - \lambda_a f_1^u + f_1^a\lambda_d^a}{f_1} = \frac{f_1^u\lambda_d^a + f_1^a\lambda_d^a}{f_1}\end{aligned}$$

which is the expression shown as Eq. (16).

Using the concept of an aggregate deposition rate, the airborne concentration of $^{214}$Pb is given analogously as

$$C_2 = \frac{\lambda_2 C_1}{\lambda_2+\lambda_v+\lambda_{d2}} = \frac{\lambda_2 C_1}{\lambda_2+r_2} \tag{17}$$

where $r_2$ is the collective removal rate of $^{214}$Pb by ventilation and deposition, and $\lambda_{d2}$ is the aggregate deposition rate of $^{214}$Pb given by

$$\lambda_{d2} = \frac{\lambda_d^u C_2^u + \lambda_d^a C_2^a}{C_2} = \frac{\lambda_d^u f_2^u + \lambda_d^a f_2^a}{f_2} \tag{18}$$

Finally, $C_3$ is equal to

$$C_3 = \frac{\lambda_3 C_2}{\lambda_3+\lambda_v+\lambda_{d3}} = \frac{\lambda_3 C_2}{\lambda_3+r_3} \tag{19}$$

where the aggregate deposition rate is given as

$$\lambda_{d3} = \frac{\lambda_d^u C_3^u + \lambda_d^a C_3^a}{C_3} = \frac{\lambda_d^u f_3^u + \lambda_d^a f_3^a}{f_3} \tag{20}$$

and $r_3$ is the collective removal rate of $^{214}$Bi by ventilation and deposition. Eqs. (18) and (20) can be obtained in a similar way that we obtained Eq. (16).

The feasibility of applying an aggregate deposition rate and the total removal rate is demonstrated by the following numerical example. Consider the following nominal input parameters: $\lambda_v=0.2\,h^{-1}$, $\lambda_a=70\,h^{-1}$, $\lambda_d{}^u=15\,h^{-1}$ and $\lambda_d{}^a=1.05\,h^{-1}$. Employing the original Jacobi model, we can obtain: $f_1=0.787$, $f_2=0.375$ and $f_3=0.234$. By applying Eqs. (16), (18) and (20), we obtained $\lambda_{d1}$, $\lambda_{d2}$ and $\lambda_{d3}$, and together with $\lambda_v$ we obtained $r_1=3.695901\,h^{-1}$, $r_2=1.699481\,h^{-1}$ and $r_3=1.267390\,h^{-1}$. Substituting these values for $r_i$ into Eqs. (15), (17) and (19), exactly the same values for $f_1$, $f_2$ and $f_3$ as the ones given by the original Jacobi model are obtained. Other input parameters will also be able to show that the aggregate deposition rate will give the true $f_i$ values.

There are now three equations, namely Eqs. (15), (17) and (19) with three known quantities, viz., $C_1$, $C_2$ and $C_3$ ($f_1$, $f_2$ and $f_3$ are also known since $C_0$ is known) and three unknown parameters,

**Table 2**
Chosen values of the parameters $\lambda_v$, $\lambda_d{}^u$, $\lambda_d{}^a$ and $\lambda_a$ (all in $h^{-1}$) and the calculated $f_i$ values with Jacobi model [18].

| $\lambda_v$ | $\lambda_a$ | $\lambda_d{}^u$ | $\lambda_d{}^a$ | $f_1$ | $f_2$ | $f_3$ |
|---|---|---|---|---|---|---|
| 0.3 | 450 | 20 | 1 | 0.8770996 | 0.4611739 | 0.2853338 |
| 0.4 | 250 | 40 | 0.6 | 0.8109253 | 0.4372427 | 0.2963494 |
| 0.8 | 150 | 80 | 0.3 | 0.6236204 | 0.2591126 | 0.1695466 |
| 1.2 | 50 | 100 | 0.1 | 0.3596369 | 0.08445625 | 0.05098491 |

viz., $r_1$, $r_2$ and $r_3$, which can be determined as

$$r_1=\frac{\lambda_1}{f_1}-\lambda_1,\quad r_2=\frac{\lambda_2 f_1}{f_2}-\lambda_2\quad\text{and}\quad r_3=\frac{\lambda_3 f_2}{f_3}-\lambda_3 \tag{21}$$

The parameters $r_i$ are known if all $f_i$ are known. On the other hand, the total removal rates $r_i$ are written as

$$r_1=\lambda_v+\lambda_{d1}=\lambda_v+\frac{\lambda_d^u f_1^u+\lambda_d^a f_1^a}{f_1} \tag{22a}$$

$$r_2=\lambda_v+\lambda_{d2}=\lambda_v+\frac{\lambda_d^u f_2^u+\lambda_d^a f_2^a}{f_2} \tag{22b}$$

$$r_3=\lambda_v+\lambda_{d3}=\lambda_v+\frac{\lambda_d^u f_3^u+\lambda_d^a f_3^a}{f_3} \tag{22c}$$

### 3.2. Determination of $f_i^u$ and $f_i^a$

The concentrations of all species of short-lived radon progeny can be calculated through the system equations of the Jacobi model given in Eqs. (12a)–(12c), if the parameters $\lambda_v$, $\lambda_d{}^u$, $\lambda_d{}^a$ and $\lambda_a$ are known. We first generate tables of test values of $f_{1,test}$, $f_{2,test}$ and $f_{3,test}$ by varying the parameters $\lambda_v$, $\lambda_d{}^u$, $\lambda_d{}^a$ and $\lambda_a$, and from these test values we can also generate test values for the total removal rates $r_{1,test}$, $r_{2,test}$ and $r_{3,test}$ through Eqs. (22a)–(22c). We then try to find the combination of parameters $\lambda_v$, $\lambda_d{}^u$, $\lambda_d{}^a$ and $\lambda_a$ that give $f_i^u$ and $f_i^a$ by minimizing the quantity $S_f$ defined as

$$S_f=(f_1-f_{1,test})^2+(f_2-f_{2,test})^2+(f_3-f_{3,test})^2 \tag{23}$$

and if necessary (see below) to also minimize the quantity $S_r$ defined as

$$S_r=(r_1-r_{1,test})^2+(r_2-r_{2,test})^2+(r_3-r_{3,test})^2. \tag{24}$$

The parameters $\lambda_v$, $\lambda_d{}^u$, $\lambda_d{}^a$ and $\lambda_a$ were varied in the ranges given in Table 1, with the following steps: the ventilation rate $\lambda_v$ was varied with steps of 0.1, attachment rate $\lambda_a$ and deposition rate of unattached progeny $\lambda_d{}^u$ were varied with steps of 1, and deposition rate of attached progeny $\lambda_d{}^a$ is varied with steps of 0.01.

Here, there are several possibilities. The first one, which is the most desired one, gave a combination of parameters that exactly reproduced the true values, i.e., $f_1=f_{1,test}$, $f_2=f_{2,test}$ and $f_3=f_{3,test}$, so $S_f=0$. However, since the parameters $\lambda_v$, $\lambda_d{}^u$, $\lambda_d{}^a$ and $\lambda_a$ were varied with finite steps, the combination of "correct" parameters might have been missed. In such circumstances, one should choose the combination where $S_f$ is the smallest. However, the situation would be complicated by the possible occurrence of more than one solution that gives the same $S_f$. In such cases, the combination that produced the smallest $S_r$ would be chosen.

Numerical examples are provided in the following to demonstrate the feasibility and correctness of this approach. Some sets of parameters were arbitrarily chosen as those shown in Table 2, and the corresponding values of $f_1$, $f_2$ and $f_3$ were calculated with the Jacobi model, which are also presented in Table 2. Here, the numerical values are intentionally given with seven digits as given by the computer (although it does not have physical sense to have such precision). A second program was then run to read the previously calculated values of $f_1$, $f_2$ and $f_3$, to vary the constants, calculate the test values $f_{1,test}$, $f_{2,test}$ and $f_{3,test}$, and finally to determine the minimal discrepancies from $f_1$, $f_2$ and $f_3$. The set of parameters that corresponded to the minimal discrepancies was then given as the results. Results corresponding to the parameters $\lambda_v$, $\lambda_d{}^u$, $\lambda_d{}^a$ and $\lambda_a$ shown in Table 2 are exactly the same as the input parameters.

**Table 3**
The parameters $\lambda_v$, $\lambda_d{}^u$, $\lambda_d{}^a$ and $\lambda_a$ (all in $h^{-1}$) obtained by minimizing $S_f$ (and $S_r$ if necessary) using the parameters in Table 2 as inputs and by truncating the $f_i$ values to three significant numbers.

| $\lambda_v$ | $\lambda_a$ | $\lambda_d{}^u$ | $\lambda_d{}^a$ |
|---|---|---|---|
| 0.29 | 449 | 20 | 1.01 |
| 0.39 | 248 | 39.7 | 0.61 |
| 0.8 | 151 | 80.6 | 0.307 |
| 1.2 | 49.48 | 99 | 0.107 |

However, in reality, $f_1$, $f_2$ and $f_3$ will not be determined with more than three significant numbers. We will here examine the potential effects of the limited accuracy of $f_1$, $f_2$ and $f_3$ on the accuracy of the determined parameters $\lambda_v$, $\lambda_d{}^u$, $\lambda_d{}^a$ and $\lambda_a$. By truncating the $f_i$ values in Table 2 to three significant numbers, the modified parameters $\lambda_v$, $\lambda_d{}^u$, $\lambda_d{}^a$ and $\lambda_a$ are shown in Table 3, which are still very close to those in Table 2. This confirms the feasibility of the method. A precaution here is that small increment steps should be used to avoid missing the correct set of parameters. The cost for this will be the long computational time.

## 4. Conclusions

In the present work, we developed the theoretical basis for long-term determination of airborne concentrations of unattached and attached radon progeny. The work was separated into two parts.

First, we showed that measurements of airborne concentrations of $^{218}$Po and $^{214}$Bi (i.e., $f_1$ and $f_3$) were possible using a stacked LR115 detector with multi-step etching. From these, the equilibrium factor $F$ and thus the airborne concentrations of $^{214}$Pb (i.e., $f_2$) could be determined.

Second, we developed the theoretical basis for the determination of the parameters of the Jacobi room model, viz., $\lambda_v$, $\lambda_d{}^u$, $\lambda_d{}^a$ and $\lambda_a$, from $f_1$, $f_2$ and $f_3$. With these parameters, the unattached fraction $f_p$ of the potential alpha energy concentration could also be determined, which facilitated more accurate determination of the absorbed dose in human lung.

## Acknowledgement

The present work was supported by a Research Grant CityU 123107 from the Research Grants Council of the HKSAR.

## References

[1] D. Nikezic, K.N. Yu, Radiat. Prot. Dosim. 113 (2005) 233.
[2] R.L. Fleischer, Health Phys. 47 (1984) 263.
[3] A.I. Frank, E.V. Benton, Nucl. Track Det. 1 (1977) 149.
[4] J.C. Hadler, S.R. Paulo, Radiat. Prot. Dosim. 51 (1994) 283.
[5] M.A. Misdaq, K. Flata, Radiat. Meas. 37 (2003) 31.
[6] K. Jamil, Fazal-ur-Rehman, S. Ali, H.A. Khan, Nucl. Instr. and Meth. A 88 (1997) 267.
[7] D. Pressyanov, J. Buysse, A. Van Deynse, A. Poffijn, G. Meesen, Nucl. Instr. and Meth. A 457 (2001) 665.

[8] D. Pressyanov, J. Buysse, A. Poffijn, A. Van Deynse, G. Meesen, Nucl. Instr. and Meth. A 516 (2004) 203.
[9] K.P. Eappen, Y.S. Mayya, R.L. Patnaik, H.S. Kushwaha, Radiat. Meas. 41 (2006) 342.
[10] R.C. Ramola, Int. Congr. Ser. 1276 (2005) 215.
[11] K. Amgarou, L. Font, C. Baixeras, Nucl. Instr. and Meth. A 506 (2003) 186.
[12] D. Nikezic, F.M.F. Ng, K.N. Yu, Appl. Radiat. Isot. 61 (2004) 1431.
[13] K.N. Yu, D. Nikezic, F.M.F. Ng, J.K.C. Leung, Radiat. Meas. 40 (2005) 560.
[14] C.W.Y. Yip, D. Nikezic, K.N. Yu, Nucl. Instr. and Meth. B 266 (2008) 5050.
[15] S.Y.Y. Leung, D. Nikezic, K.N. Yu, J. Environ. Radioact. 92 (2007) 55.
[16] S.Y.Y. Leung, D. Nikezic, J.K.C. Leung, K.N. Yu, Appl. Radiat. Isot. 65 (2007) 313.
[17] D. Nikezic, K.N. Yu, Radiat. Environ. Biophys. 40 (2001) 207.
[18] W. Jacobi, Health Phys. 22 (1972) 441.